

LASERS

PACS numbers: 42.55.Rz; 42.60.By; 42.60.Da; 42.60.Lh; 42.65.Yj
DOI: 10.1070/QE2014v044n05ABEH015437

Optimisation of wide-band parametric amplification stages of a femtosecond laser system with coherent combining of fields

S.N. Bagayev, V.I. Trunov, E.V. Pestryakov, V.E. Leshchenko, S.A. Frolov, V.A. Vasiliev

Abstract. **For the first time the pulses with the energy of ~150 mJ and the spectrum corresponding to the transform-limited duration of ~20 fs amplified in three-stage parametric amplifiers have been coherently combined in a dual-channel femtosecond laser system. The efficiency of coherent combining of above 90% has been obtained at the residual relative time jitter of amplified pulses of 110 as. For the first time the modulation of spectrum was experimentally observed under the parametric amplification of a wide-band femtosecond radiation in crystals placed in series. The model of parametric luminescence evolution was developed which allows one to calculate the whole range of the frequency-angular spectrum that, in addition to simulations of the contrast of amplified pulses, gives the possibility of optimising the amplifier efficiency. The results of experiments on measuring the contrast are presented and compared with the calculated data. Methods for enhancing the contrast in the created laser system are analysed. Possible schemes of multibeam pumping of the output cascade are considered for obtaining a petawatt power in the laser system based on cascades of a parametric amplifier in LBO crystals which is being developed at the Institute of Laser Physics of SB RAS.**

Keywords: *petawatt laser system, parametric amplification, coherent combining, multi-beam pumping, femtosecond pulses, contrast.*

1. Introduction

Development of optical parametric chirped-pulse amplification (OPCPA) opens ways for creation of a new kind of super-high-power laser sources with extremely short pulse duration and intensity greater than 10^{23} W cm^{-2}. Obtaining such intensities will make it possible to study experimentally numerous effects of ultra-relativistic optics [1].

Investigations performed at the Institute of Laser Physics of the Siberian Branch of the Russian Academy of Sciences concern the development of principles for generating extreme light fields and creating the multichannel femtosecond laser system of ultra-relativistic intensity based on the method of coherent combining of femtosecond pulses amplified by using the OPCPA method under picosecond pumping. The possibility of obtaining a sub-petawatt peak power of amplified pulses in a single-channel system with nanosecond pumping was demonstrated in [2, 3]. Presently, only the method of coherent combining allows one to overcome limitations on the aperture of amplifiers and compressors and to increase noticeably a highest attainable peak power of laser pulses [4]. Up to now in the framework of the developed laser system, two channels of three-stage parametric amplification are created with the pulse energy in each channel of up to 150 mJ and the efficiency of subsequent coherent combining above 90%. A detailed description of the system realised is given in Section 2.

Later the energy of pulses will be increased by adding output stages, which along with the employment of the developed stretcher–compressor system [5] will provide a petawatt level of peak power.

In developing the system, much attention was paid to the choice of the scheme for the first amplifying stage. In the first stage, the gain of ~10^6 and high contrast are required, which causes one to choose between a single-pass scheme with two crystals and a two-pass scheme with one crystal. This problem is considered in Section 3.

Note that the contrast of amplified pulses is of principal importance in developing high-intensity femtosecond systems. The contrast is the key parameter in such systems because a low contrast may result in undesirable effects, for example, in producing plasma by a pre-pulse [6].

The contrast of the pulse of the laser system based on parametric amplification is related to a number of factors, the main among which is amplified parametric luminescence. A series of papers have been published concerning experimental investigations and optimisation of the contrast of pulses in high-power laser systems with parametric amplification cascades [7, 8]. A maximal contrast obtained with plasma mirror and cross-polarised waves is ~10^{-10} [9]. A drawback of this approach is complexity and a lower energy of amplified pulses. Hence, the problem of increasing the contrast of output pulses in parametric amplification cascades is still urgent. In Section 4 we consider various aspects of evolution and suppression of parametric luminescence amplification and the model of superluminescence development in parametric amplification is suggested with the allowance made for diffraction, double refraction, dispersion of group velocities, and saturated amplification, which makes it possible to calculate the frequency-angular spectra of superluminescence; methods for enhancing the contrast are suggested and analysed.

Simulations show that obtaining a petawatt output power at final amplifying stages of the system developed requires a considerable energy of a picosecond pump pulse [10], which can hardly be realised in a single-beam system. For solving

S.N. Bagayev, V.I. Trunov, E.V. Pestryakov, V.E. Leshchenko, S.A. Frolov, V.A. Vasiliev Institute of Laser Physics, Siberian Branch, Russian Academy of Sciences, prosp. Akad. Lavrent'eva 13/3, 630090 Novosibirsk, Russia; e-mail: trunov@laser.nsc.ru

Received 3 March 2014; revision received 24 March 2014
Kvantovaya Elektronika **44** (5) 415–425 (2014)
Translated by N.A. Raspopov

the problem we suggest the multi-beam pumping, optimal schemes for which are given in Section 5.

2. Three-stage two-channel laser system based on parametric amplification

Presently, the two-channel femtosecond laser system with three cascades of parametric amplification in each channel and coherent combining of amplified pulses is created at the ILP SB RAS. The scheme of the experimental setup is shown in Fig. 1. A Ti:sapphire femtosecond laser (FemtoLasers) is used as a seed laser, which generates the pulses with a centre wavelength of 800 nm, duration of 10 fs, and pulse repetition rate of 75 MHz. Then femtosecond pulses are stretched to ~50 ps in a two-pass grating stretcher comprised of two gold-coated holographic gratings HoloGrate (JSC) 1200 lines mm^{-1}; the distance between the gratings is ~54 mm. Efficient parametric amplification is only possible under the optimal overlapping of the pump and amplified pulses in a nonlinear crystal. The system developed for synchronising the femtosecond laser and the driving picosecond laser of the pump system provides the relative instability of pulses (jitter) of the lasers at the level of less than 200 fs [11].

A four-channel APL 2106 (Ekspla) pump laser generated in each channel the pulses with the energy of up to 600 mJ and duration of 90 ps at the pulse repetition rate of 10 Hz and the beam diameter of approximately 16 mm at the e^{-2} level. The amplified pulse was selected by rotating its plane of polarisation by 90° with the help of the pulse picker OG8-1 (Avesta), synchronised with the pump laser.

Optical parametric chirped-pulse amplifiers are based on BBO (β-BaB_2O_4) and LBO (LiB_3O_5) nonlinear crystals. The first cascades are realised according to the two-pass amplification scheme on BBO crystals (type I, $\theta = 23.7°$, $\varphi = 90°$, the length is 5 mm, the aperture is 8×8 mm), the second and third cascades are based on the single-pass scheme. In the second stage of the first channel, an LBO crystal (type I, $\theta = 90°$, $\varphi = 13.8°$, with the length of 9 mm and aperture of 18×18 mm) is used, whereas in the second stage of the second channel, use is made of a BBO crystal (type I, $\theta = 23.7°$, $\varphi = 90°$, with the length of 3.5 mm and aperture of 18×18 mm). In the third stages the amplification occurs in LBO crystals (type I, $\theta = 90°$, $\varphi = 13.8°$, with the length of 4.3 mm and aperture of 30 mm). Since the quality of the pump hyper-Gaussian beam worsens as it propagates, maintaining the initial quality requires the image relaying from the output of the pump laser to the nonlinear crystal. For this purpose an evacuated image-relay two-lens telescope with minimal divergence is used. In this case in the first stages the beam diameter is reduced to 3.5 mm, in the second stages – to 13 mm, and in the third stages it is kept at the level of 16 mm. After the first cascade, the beam of amplified radiation of diameter ~2 mm is expanded by the telescope to ~15 mm for matching with the diameter of the pump beam in the second stage.

In the first channel the energy of amplified pulses after three stages was 150 mJ, in the second channel it was 160 mJ. The characteristic root-mean-square instability of amplified pulses was ~3%. The energies of pump and amplified pulses in different stages are given in Table 1 for both channels. Spectra of amplified pulses are shown in Fig. 2. The angular instability of amplified pulses found from recorded fluctuations of the position of beam centre-of-mass in the focal plane of spherical mirror was 13 μrad in the first channel and 15 μrad in the second channel at the recording duration of 100 s. The FWHM divergence of amplified pulses was 90 μrad at the beam diameters of 11 mm.

Table 1. Energies of pump and amplified pulses.

Stage number	Energy of pump pulses/mJ		Energy of amplified pulses/mJ	
	channel 1	channel 2	channel 1	channel 2
1	31	34	3	1.4
2	470	360	100	100
3	430	504	150	160

According to simualtions, the increase in the energy of pump pulses in the second and third stages up to 600 mJ may raise the output energy of amplified pulses to 340 mJ.

The coherent combining of amplified pulses was performed in the focal plane of the spherical mirror with the radius of curvature $R = 3$ m. The relative jitter needed for coherent combining was stabilised by the system described in [4, 11]. The profiles of beams in the focal plane were recorded by a Spiricon L11058 CCD camera (with a pixel size of 9×9 μm) after preliminary attenuation. Characteristic profiles of amplified and combined pulses are shown in Fig. 3.

The efficiency of coherent combining calculated for a series of recorded profiles (each of duration ~10 s) determined by the expression

$$\eta = I_\Sigma [I_1 + I_2 + 2\sqrt{I_1 I_2}]^{-1}, \quad (1)$$

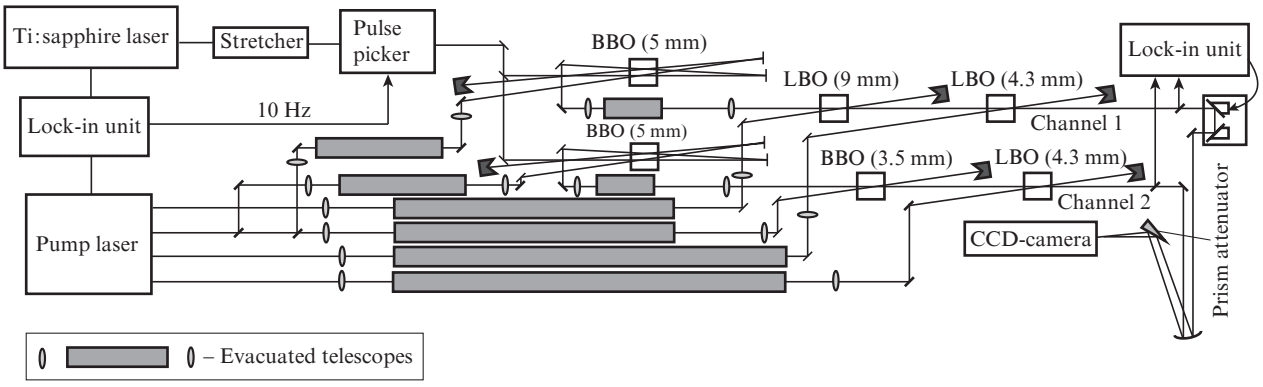

Figure 1. Experimental setup.

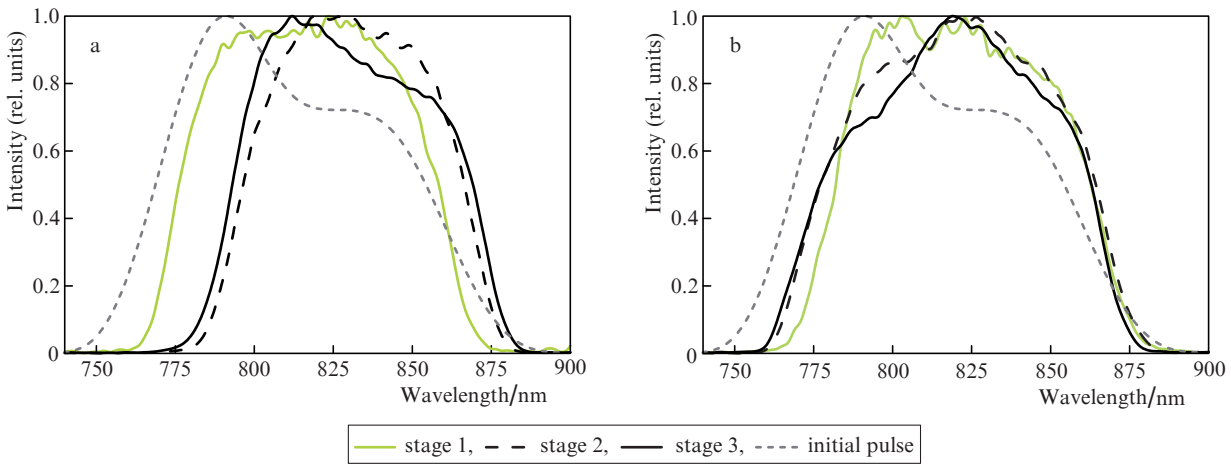

Figure 2. Spectra of initial and amplified pulses in (a) the first and (b) second channels.

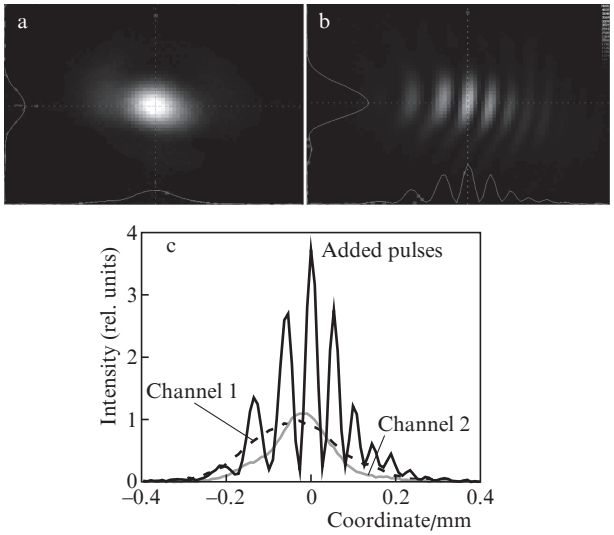

Figure 3. Profiles of (a) single and (b) combined pulses and (c) horizontal projections of all profiles in the focal plane of a spherical mirror with $R = 3$ m.

was 93 ± 3%. Here, I_1, I_2, and I_Σ are the peak densities of energy for the amplified pulses in the first and second channels and for the combined pulse.

In this case the accuracy is mainly determined by the instability of energy of pulses. Note that due to slightly different spectra of amplified pulses in the channels, the maximal feasible efficiency of the combining determined by expression (2) would not be greater than 98%:

$$\eta = \frac{1 + 2\int \sqrt{I_1(\omega) I_2(\omega)}\, \mathrm{d}\omega / A}{1 + 2\sqrt{\int I_1(\omega)\, \mathrm{d}\omega \int I_2(\omega)\, \mathrm{d}\omega}\, / A}, \qquad (2)$$

where

$$A = \int I_1(\omega)\, \mathrm{d}\omega + \int I_2(\omega)\, \mathrm{d}\omega;$$

$I_1(\omega)$ and $I_2(\omega)$ are the spectra of amplified pulses; and ω is the radiation frequency.

According to the analysis [4, 11] the residual jitter for the time of the order 110 as between amplified pulses reduces the efficiency of coherent combining to 97%. The angular instability of ~14 μrad with the angular spectra measured (Fig. 3) additionally reduces the efficiency to ~91%.

One more important factor affecting the efficiency of coherent combining is a spectral phase difference of combined pulses. In the present work the spectral phase of amplified pulses was not controlled. However, the spectral difference of phases of amplified pulses may be non-zero due to the employment of different crystals in the second stage and to uncontrolled dispersion of mirrors. This factor was experimentally minimised by introducing glass plates of varied thickness into the second channel. The optimal value was determined by a maximal efficiency of coherent combining with the adjustment step of ~45 fs^2 (K8 glass of thickness ~1 mm). The accuracy of matching the dispersions with such a step value taking into account the experimentally recorded spectra of amplified pulses should provide a maximal efficiency with the inaccuracy no worse than 1% [4].

Thus, the echieved efficiency of coherent combining agrees with the theoretical expectations based on measured instabilities of combined pulses. The main limitation at this step is the angular instability of amplified pulses which forced us to design the system for angular stabilisation of output radiation and thus enhance the efficiency of coherent combining and improve the stability of peak intensity of all the pulses.

We developed the stretcher–compressor system for compressing amplified pulses, which is capable of compressing pulses of a petawatt (and higher) power level [5] in the system under consideration. The further tight focusing of compressed pulses will provide the intensities of ~10^{20} W cm^{-2} which opens the possibilities for further investigations in the field of relativistic optics.

3. Wide-band parametric amplification in crystals placed in series

Optimisation of parameters of the first stage is an important factor for obtaining a maximal-contrast and high-quality beam in the multistage laser system based on parametric amplification. Employment of a long (~10 mm) BBO crystal in the first stage of the single-channel scheme provides consid-

erable amplification of parametric luminescence. A two-pass scheme makes the energy of amplified parametric luminescence lower; however, the problem arises related to difficult realisation of high spatial quality of the pump in both passes because it not possible to relay the image to the passes simultaneously. In turn, the scheme with two crystals placed in series solves the problem because a short distance between the crystals helps to keep the quality of the pump beam close to that of the image. In addition, although the scheme does not solve the problem of high-energy luminescence, it may compensate for birefringence and separate phase-matching of each crystal for an optimal gain spectrum.

Placement of nonlinear crystals in series in nonlinear conversions has been considered earlier. The influence of the additional phase caused by a gap between the crystals on the efficiency of second harmonic generation [12] and spectrally narrow parametric amplification [13] has been studied.

We have studied the influence of the gap between the crystals on the parameters of amplified wide-band radiation. It was found that at a sufficiently small gap where the idler wave has no time to leave the domain in which signal and pump overlap, the spectrum of the wide-band amplified pulse becomes modulated.

The modulation is caused by the phase sensitivity of parametric amplification. A phase difference arises between the beams as they propagate across the crystal and the gap which is related both to dispersion and diffraction and to noncollinearity of the beams. In amplification of wide-band pulses the determining, as a rule, is noncollinearity, whereas contributions of other factors are noticeably smaller. This effect has not been observed in the papers mentioned above because of a small bandwidth of radiation spectra.

It is important that the modulation only arises when the signal and idler waves overlap in the domain of amplification in the second crystal, because without it the phase difference between the signal and pump would transfer to a new idler wave.

The simple model of parametric amplification based on truncated equations [14] makes it possible to estimate the modulation period. Parametric amplification is most efficient when the phase differences between waves (pump φ_p, idler φ_i, and amplified φ_s) satisfy the condition [14]

$$\Delta\varphi = \varphi_p - \varphi_s - \varphi_i = \pi/2. \quad (3)$$

The interacting beams propagating between the crystals acquire different additional phase incursions. In the second crystal most efficiently amplified will be the components satisfying relationship (3) and least efficient will be the components whose total phase in the left side is $-\pi/2$. From (3) follows that the modulation period can be calculated from the following condition on the phase difference:

$$\Delta\varphi = \frac{L}{c}\left[\omega_p - \omega_s\cos\alpha - \omega_i\cos\frac{\omega_s}{\omega_i}\alpha\right] = \frac{\pi}{2} + 2\pi n, \quad n \in \mathbb{Z}, \quad (4)$$

where L is the length of air gap; c is the speed of light in vacuum; ω_p, ω_s, and ω_i are the frequencies of the pump, amplified, and idler waves, respectively; and α is the external angle of noncollinearity. Thus, the modulation period depends on the frequency, external noncollinearity angle, and length of the air gap. An analysis shows that the strongest dependence is determined by the last two factors.

In order to experimentally study the considered effect we have performed a series of experiments with parametric amplification in two BBO crystals placed in series (type I, θ = 23.7°, φ = 90°, the thickness is 5 mm, the aperture is 8 × 8 mm). The experiments have been performed on the first stage of the scheme shown in Fig. 1, slightly modified for obtaining single-pass amplification in the two-crystal variant.

The dependences of the modulation period on a distance between crystals, calculated from expression (4) and measured experimentally, are shown in Fig. 4. The period was experimentally found from a set of the modulation peaks whose intensity was at least half the maximal intensity. For comparing with theoretical values, the same spectral range was used as in the experiments. This method for determining the modulation period makes allowance for its frequency dependence and reduces the inaccuracy due to profile fluctuations of experimental spectra. In Fig. 4 one can see that the calculated and experimental periods of modulation coincide with a high accuracy.

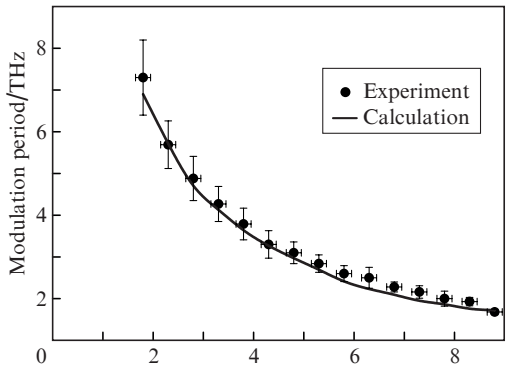

Figure 4. Modulation period of spectrum versus the distance between crystals.

Experimental data show that the modulation depth depends on the distance between the crystals in recording both the integral angular spectrum and spectrum in a narrow angular range (Fig. 5a). The reduction of the modulation depth in the spectrum integrated over angle can be explained by the partial shift of the idler wave from the interaction zone (the shift in our case is 1.3 mm per 1 cm of gap length), and by divergence of the beams. In the latter case the phase of modulation slightly changes and the averaging reduces the modulation depth due to shifts of minima for different angular components. Nevertheless, in a simple model none of these factors explains the partial modulation in the spectrum for the narrow angular range of the amplified beam as shown in Fig. 5a. The phenomenon is explained if the linear effects are taken into account such as dispersion of group velocities, diffraction, and double refraction, which violate phase relationship (3) already in the process of amplification in the second crystal.

According to our improved model of parametric amplification described in [15] the allowance made for the experimentally measured divergences of pump and amplified beams (~1 mrad each) makes it possible to correctly calculate the modulation depth. Dependences of experimentally measured and numerically modelled modulation depths as functions of the distance between crystals are shown in Fig. 5b. Numerous factors affecting the modulation depth, for example, the shapes of the angular spectrum of pump and amplified radiation, the degree of saturation, result in a worse agreement with calculations. A detailed study of the problem reveals that the determining factor is the divergence of the pump beam because in our conditions it low-

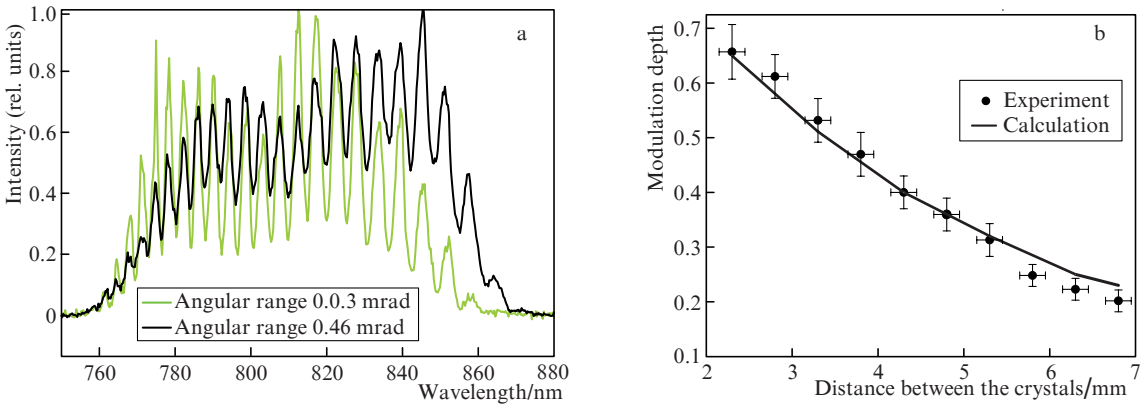

Figure 5. (a) Experimentally measured spectra in the case of amplification in different angle ranges at the distance between crystals placed in series of 6.3 mm and (b) the comparison of calculated and experimental depths of spectrum modulation versus the length of the air gap.

ers the modulation depth by almost four times more efficiently than the divergence of the amplified beam.

One more specific feature of employing two crystals placed in series is that the efficiency of amplification falls almost twice just at a distance between the crystals of several hundred microns. A calculated energy of the amplified pulse is shown in Fig. 6 versus the distance between the crystals. One can see that at the air gap of above 100 μm the energy of the amplified pulse sharply falls (by almost 1.7 times at 550 μm where a gain minimum is close to a centre of the pulse spectrum). A further weak increase in the energy at distances of ~850 μm is related to a reduction of the modulation period to the value less than the spectral width of the amplified pulse; the following slow fall is explained by a divergence of the signal and pump in space.

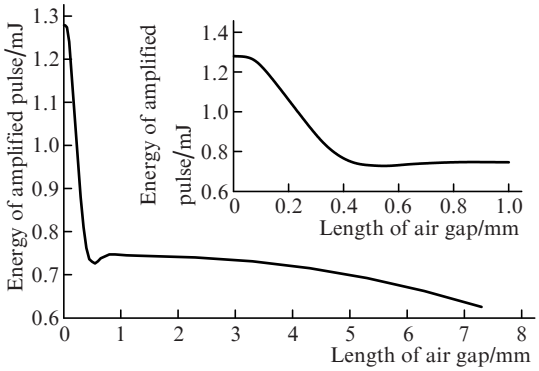

Figure 6. Calculated dependence of the energy of amplified pulse vs. the length of air gap. The inset shows the enlarged fragment of the curve in the range 0–1 mm.

Thus, amplification in two crystals placed in series without blocking the idler wave not only results in the modulation of the spectrum structure but also worsens the amplification efficiency, which as a whole makes this scheme of little use for amplifying ultrashort femtosecond pulses.

4. Parametric luminescence and contrast in parametric amplification

By now a number of models are suggested and analysed in works devoted to the methods for simulating amplification of parametric superluminescence, which, however, have certain limitations and drawbacks. For example, the model [8] for calculating the contrast of chirped pulses requires some empirical data, which can only be obtained on an operating laser system. In addition, all previously suggested models for calculating the contrast either require a huge RAM on a computer [8, 16, 17] or cannot describe some spatial effects [17].

4.1. Model of parametric luminescence evolution

We have developed the model of superluminescence evolution in parametric amplification with diffraction, double refraction, dispersion of group velocities, and saturated amplification taken into account, which simulates the frequency-angular spectra of superluminescence. The model is based on separating two stages in amplification of luminescence. The first stage in which the number of luminescence photons is small and corresponds to an initial period of amplification can be referred to as ‘quantum’. The second stage is ‘classical’: the number of photons per mode is much greater than unity.

At the ‘classical’ amplification stage, well known truncated equations are valid [14] whereas the ‘quantum’ stage requires distinct consideration. Having analysed a number of methods for solving this problem we chose the approach based on so called Wigner stochastic method, which reduces the quantum consideration of the evolution of spectral density of photon distribution to a classical consideration of the evolution of a set of initial states [18]. At the first stage, a set of the initial states of photons is chosen assuming that there is a single photon per mode which can be treated as the density of zero fluctuations of electromagnetic vacuum [19]. Numerically such states are given by complex white Gaussian noise. Solution of the classical equations for a set of states allows one to find a set of the final states which, being averaged, give the average number of photons. Finally, both ‘classical’ and ‘quantum’ amplification stages are described by classical equations {see, for example, (1) in [15]}.

The equations describing evolution of luminescence were derived according to formalism from [15]: the wave field was presented as a sum of the main wave and luminescence wave, then this sum was substituted into the system of truncated equations {see formula (1) in [15]} and linearization over the weak luminescence wave was performed. For simplicity, we supposed that the main waves have a narrow frequency-angular spectrum at a prescribed point in space and time (this con-

dition almost always holds in OPCPA). The final system of equations used for describing the evolution of luminescence is sufficiently cumbersome. It comprises six similar equations, one of which looks as follows:

$$\frac{\mathrm{d}A_{\mathrm{s1}}}{\mathrm{d}z} = \mathrm{i}\left(\frac{k_{\mathrm{s1}}}{\cos k_{\perp}/k_{\mathrm{s1}}} - k_{\mathrm{s0}} - \frac{\omega_{\mathrm{s1}} - \omega_{\mathrm{s0}}}{v_{\mathrm{grp}}}\right)A_{\mathrm{s1}}$$

$$-\mathrm{i}\sigma_{\mathrm{s}}(A_{\mathrm{p0}}A^{*}_{\mathrm{i2}} + A_{\mathrm{p1}}A^{*}_{\mathrm{i0}})\exp(\mathrm{i}\Delta kz), \qquad (5)$$

where the index m = s, i, p corresponds to the signal, idler, and pump waves; the index j = 0, 1, 2 with zero corresponding to the main wave, 1 and 2 corresponding to angular components of luminescence with the zero sum of projections of wave vector onto the plane normal to the z axis; A_{m0} is the envelope of the electric field strength for the main wave; A_{mj} is the spectral distribution of photons over modes (j = 1, 2); σ_m is the coefficient of second-order nonlinearity; ω_{mj} is the frequency; ω_{m0} is the frequency of carrier; k_{mj} is the wave vector; v_{grp} is the pump group velocity; and Δk is the wave mismatch. To transfer from the number of photons in modes to the intensity, A_m is multiplied by the spectral 'vacuum brightness' $S^{\mathrm{vac}}_{\omega\Omega} = \hbar\omega^3/(8\pi^3c^2)$ (W Hz^{-1} sr^{-1} cm^{-2}) [19] and integrated over frequencies and angles.

System (5) describes evolution of frequency and angular distributions of photons in parametric amplification at a prescribed point in space and time. For obtaining the intensity distribution of superluminescence in our model it is necessary to perform calculations for a set of spatial coordinates of the beam (usually it suffices 5–10 points). On the other hand, the developed model gives a possibility to calculate the luminescence spectrum in a wide range of frequencies regardless of a chosen spatiotemporal resolution for main waves, which substantially weakens requirements to the amount of RAM. Generally, one may perform calculations which would be difficult with other models. In particular, the possibility to calculate the whole frequency-angular spectrum of luminescence allows one to estimate the total energy of luminescence, hence, opens prospects for developing the methods for limiting its influence on the energy of amplified pulse. To our knowledge, the model with mentioned features is suggested for the first time.

4.2. Measurement and optimisation of contrast in a three-stage laser system

The model of parametric luminescence evolution developed in the present work was verified by a series of experiments using a two-pass parametric amplifier based on a BBO crystal (with the length of 8 mm, phase-matching angle of 23.7°, internal noncollinearity angle of 2.3°). The pump energy (with a centre wavelength of 532 nm) of the cascade was 10–30 mJ at the pulse duration of 90 ps and the beam radius (at the level e^{-2}) of about 2 mm. The initial energy of the amplified pulse (with the centre wavelength of 800 nm) was ~1 nJ, the pulse duration prior to stretcher was 10 fs, and after the stretcher it was 8 ps. The amplified pulse was compressed in the bulk compressor based on two blocks from glass TF10 and K8 of lengths 140 and 90 mm, respectively. In our conditions, the amplified compressed pulse had the energy of 50–100 μJ and duration of about 50 fs at the transform-limited pulse duration of 20 fs. The increased duration is explained by the fact that the volume compressor employed and the grating stretcher have equal signs of the third-order dispersion which total value is ~60000 fs^3; in view of the width of the recorded spectrum this increases the duration to ~50 fs. Note that the uncompensated dispersion will affect the results of contrast measurements only in time lapses of several picoseconds at most [20]. Since we deal with periods comparable with the pump duration (dozens of picoseconds) we may neglect the influence of uncompensated dispersion in analysing data obtained. The contrast of amplified pulses was measured with a COMET 800-2 contrast meter (Avesta Project Ltd.) having the time range of 950 ps and maximal dynamic range of 10^9.

Results of measurements and calculations of the contrast of amplified pulses are shown in Fig. 7 for two delays between the amplified and pump pulses. One can see that the model developed at a high accuracy describes experimental data and can be used for optimising the parameters of the laser system developed. The results presented show that optimisation of the delay between the pump and amplified pulses may improve the contrast which was also demonstrated in [21, 22].

Based on the model developed we calculated the expected contrast of the three-stage system. An important factor determining the contrast of the system as a whole is the contrast of pulses of the driving femtosecond laser. According to [23] the contrast of a Ti : sapphire laser is about 10^{-8}.

In our simualtions the contrast of pulses of femtosecond laser was modelled similarly to the approach to zero fluctuations of vacuum except for the fact that the frequency-angular spectrum of the amplified pulse coincided with that of the main pulse. Calculations show that at the initial contrast of 10^{-8} its resulting value after amplification is comparable to the contrast progressed from zero fluctuations. Hence, in our conditions the effective contrast value related to parametric superluminescence is 10^{-8}.

As was mentioned, the contrast of the leading edge of the amplified pulse may be improved at the sacrifice of worsening the contrast of the trailing edge by optimising the delay between the amplified and pump pulses; a maximum of the signal pulse should be shifted forward relative to maximum of the pump pulse (see Fig. 7). In our case this is determined by the Gaussian time profiles of pump pulses – in shifting the signal forward the pump intensity near its leading edge will be lower. However, a superfluous increase in the delay will reduce the efficiency of amplification of the signal wave and, hence, worsen the total contrast. Note that the efficiency of this method depends on a number of factors. For example, it is most efficient at a high gain in the case of saturation; however, with the hyper-Gaussian time profile of the pump the effect will be minimal or absent. In this case the duration of the stretched pulse should be chosen such that it would overlap the pump pulse. For obtaining a maximal contrast of amplified pulses each particular configuration of the system should be optimised by numerical modelling.

One more possibility to enhance the contrast is to optimise the saturated amplification. For example, amplification in the regime of inverse energy transfer from signal to pumping substantially worsens the contrast despite the increase in the spectral width of the amplified pulse. This effect is explained by the nonuniform reduction of the pump intensity under saturation, and with the Gaussian time profiles of signal and pump the most noticeable fall of intensity (down to zero) will be observed at the centre of the pump pulse, whereas at the edges the intensity will be kept at a higher level. This will result in a greater (as compared to the amplification of the pulse as a whole) amplification at edges of signal spectra (which is chirped in the considered case) and luminescence. In approaching a maximum of the energy of the amplified pulse

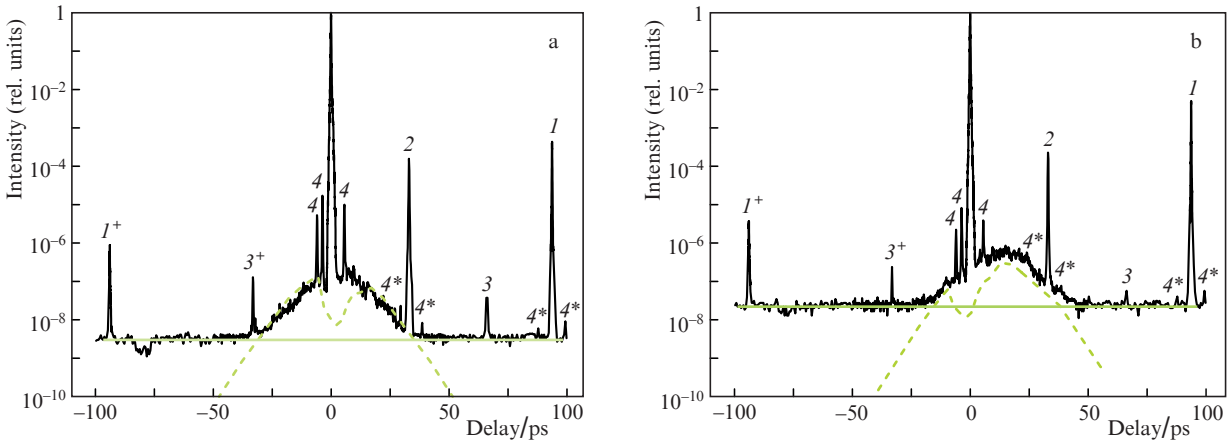

Figure 7. Comparison of the measured contrast for two delays differing by 20 ps (solid curves) with calculated data (grey dashed curves). Solid grey curves show the noise level of the recording system. The following artifacts are marked: (*1*) (93.6 ps) pulse reflection from faces of the crystal of length 8 mm; (*2*) (33 ps) reflection from faces of the attenuator of the contrast meter; (*3*) secondary reflection from faces of the attenuator of the contrast meter; (*4*) reflection from crystal faces of second and third harmonics of the contrast meter; asterisk denotes the repeating artifacts due to reflection, plus refers to the artifacts caused by specific features of the cross-correlation function due to the post-pulses arisen from reflections.

with the Gaussian profile of the pump, the contrast also falls; nevertheless, this effect is usually weak and can be to a high degree suppressed by the choice of the delay between the amplified and pump pulses. Obviously, the effects of broadening the spectrum of the amplified pulse and worsening the contrast would become weaker as the shapes of signal and pump pulses approach a staircase waveform.

The dependences discussed above are illustrated in Fig. 8 where a calculated contrast of the amplified pulse is shown for three stages of our laser system at two different delays and various saturation levels.

As follows from the calculations, the best contrast is attained at the following parameters: the delay between signal and pump pulses is 20 ps (a 30-fold increase in the contrast), amplification of up to 80% of the maximal energy at the first stage (approximately a three-fold enhancement) (Fig. 8e). In the whole, optimisation enhances the contrast by approximately three orders of magnitude from 3×10^{-6} (Fig. 8b) to 10^{-8} (Fig. 8e). In this case, the energy reduced in the second stage due to saturated amplification is compensated for in the third stage so that the output energy of the amplified pulse is reduced by less than 3% and the pulse duration is increased by at most 15%.

Thus, in optimising the developed system one may expect the contrast on the order of 10^{-8} which is comparable to the value obtained in [21, 23] for systems based on parametric amplification. The developed system can be scaled up to petawatt and multi-petawatt levels [4] with the contrast of about 2×10^{-8}. The contrast in our system can be further enhanced by optimising the first amplifying stage using known methods for generating cross-polarised waves and plasma mirror [9].

5. Optimisation of output stages of laser systems based on parametric amplifiers with multi-beam pumping

For increasing the peak power in the channels of the developed system to the petawatt level it is important to lower the requirements to the pulse energy of lasers pumping output cascades [4] which can be realised by using schemes of multi-beam pumping. This method has been employed in a number of works in recent years. For example, five pump beams have been successfully employed [24] for spectrally narrow amplification in a LBO crystal with noncritical phase matching. The possibility of employment of coherent [24–26] or incoherent [27] (with different wavelengths) multi-beam pumping was demonstrated. In the latter case, the output energy can be increased in view of the fact that the limiting added density of energy in a nonlinear crystal is attained at higher individual pump intensities. In that case, pairs of pump beams are in different planes at the angular distance from each other sufficient for suppressing parasitic amplification.

One more possibility to employ several pump beams is to increase the gain bandwidth due to different noncollinearity angles and phase matching [26]; however, the amplification efficiency is substantially reduced in this case. In [26] the efficiency was several times less than the maximal value feasible with the system parameters used in that work, which is related with the competition of idler waves at different wave mismatch [28]. This is a typical situation in broadband amplification in the case of different phase matching angles and noncollinearity angles, whereas at a small amplitude of the idler wave in some spectral range, for example, in the range of substantial wave mismatch, the wave competition weakens. In this case, however, the pump intensity will not fall because saturation is absent, which, as shown in a previous section, will result in a substantial degradation of the contrast. In what follows we will consider the multi-beam pumping in the context of obtaining high amplification efficiency at a minimal elongation of pulse durations in the amplification process which implies almost complete coincidence of the gain profiles provided by each pump and, hence, a small difference between wave mismatches in the spectral range of amplification.

In analysing the possibility and conditions for realising the multi-beam pumping, a model based on equations (1) from [15] has been developed. It differs from (1) in that instead of one there are N pump waves and N idler waves, which can be considered as the separate fields each residing in its particular frequency-angular domain. These domains for different pump and, correspondingly, idler waves do not overlap because the divergence of beams in our case is dozens of

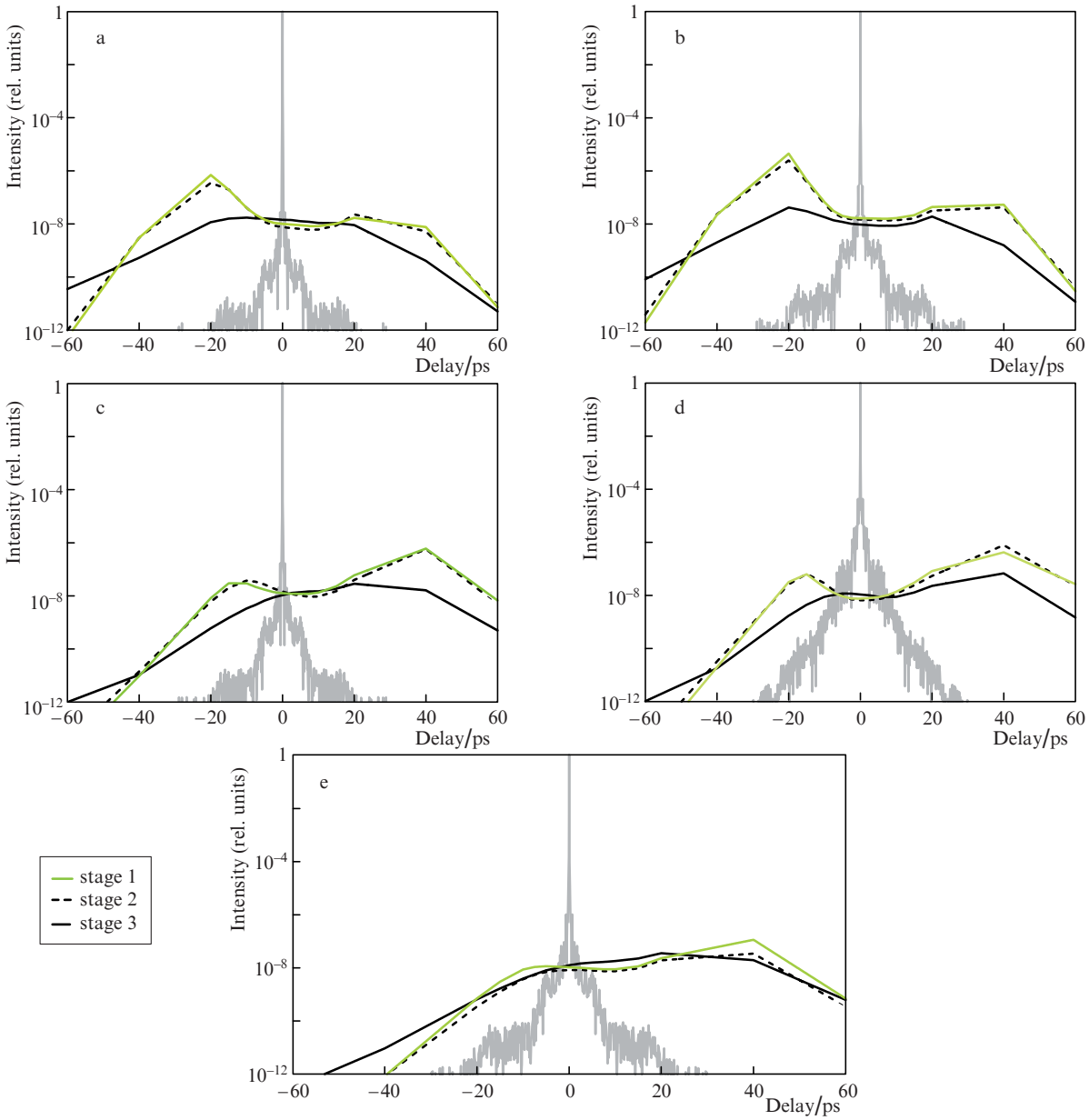

Figure 8. Calculated contrasts of pulses for three stages of the laser system developed:
(a) amplification is 80% of the maximal energy in the first stage and the maximal energy in the rest stages at zero delay; (b) amplification to the maximal energy in all the stages at zero delay; (c) same as (a) but the delay is 20 ps; (d) same as (b) but the delay is 20 ps; (e) the contrast optimised similarly to (c) but with the second-stage amplification of 90% of the maximal energy.

microradians, whereas the angles between the beams are 7 mrad and more. The system of equations for N pump beams is as follows

$$\frac{\partial A_\mathrm{s}}{\partial z} = \hat{L}_\mathrm{s}^{(\mathrm{s})} A_\mathrm{s} + \mathrm{i}\sum_{j=1}^{N} \sigma_{\mathrm{s}j} A_{\mathrm{i}j}^{*} A_{\mathrm{p}j} \exp(\Delta k_j z),$$

$$\frac{\partial A_{\mathrm{i}j}}{\partial z} = \hat{L}_{\mathrm{i}j}^{(\mathrm{s})} A_{\mathrm{i}j} + \mathrm{i}\sigma_{\mathrm{i}j} A_\mathrm{s}^{*} A_{\mathrm{p}j} \exp(\Delta k_j z),$$

$$\frac{\partial A_{\mathrm{p}j}}{\partial z} = \hat{L}_{\mathrm{p}j}^{(\mathrm{s})} A_{\mathrm{p}j} + \mathrm{i}\sigma_{\mathrm{p}j} A_{\mathrm{i}j} A_\mathrm{s} \exp(-\Delta k_j z), \qquad (6)$$

$$\hat{L}_m^{(\mathrm{s})} A_m = \mathrm{i}F_{-}\left[\left(\frac{k_m}{\cos(k_\perp/k_m)} - k_{m0} - \frac{\omega_m - \omega_{m0}}{v_\mathrm{grs}}\right)F_{+}[A_m]\right],$$

$$\Delta k_j = k_{\mathrm{p}j0z} - k_{\mathrm{s}0z} - k_{\mathrm{i}j0z},$$

where v_grs is the group velocity of the signal wave; Δk_j is the mismatch of the wave in the interaction with a pump wave j; and σ_{mj} is the coefficient of second-order nonlinearity for wave m interacting with wave j. The rest notations are similar to (1) from [15] except for m = s, ij, pj, where the first indices have been defined earlier and index j corresponds to a pump wave; $\hat{L}_m^{(\mathrm{s})}$ is a linear operator similar to that in (1) from [15].

An important point is the threshold pump intensity. If N pump beams are coherent and have equal intensities then their net peak density of energy will raise as N^2. Hence, in increasing the number of the pump beams it is necessary to reduce their intensities in accordance with the quadratic dependence on their number. On the other hand, if they are not coherent (different wavelengths), then their intensities should be reduced as N^{-1}. However, in the case of close wave-

lengths the total intensity is proportional to N only in averaging and the instantaneous intensity will be determined by a continuous series of the pulses with the duration corresponding to the difference of frequencies and with the intensity proportional to N^2. In this situation it is not possible to judge whether it would result in a breakdown without thorough theoretical and experimental analysis. All this requires an additional study. However, in what follows we consider the case of incoherent pump beams as optimal.

Note that the increase in the intensity of pump beams in the crystals necessitates greater transverse dimensions of the crystals; hence, schemes with multi-beam pumping require crystals of greater dimensions than schemes with series amplifying cascades. Thus, according to the analysis performed, in pumping by six beams the needed increase in the crystal transverse dimension is from 20% (at equal energies of amplified and pump pulses) to 70% (in the case where the energy of the amplified pulse is noticeably less than that of the pump). Nevertheless, a substantial advantage of the multi-beam pump scheme is that it realises a higher efficiency and gain bandwidth due to a higher peak pump intensity; consequently, a higher peak power of the amplified pulse can be obtained.

For obtaining a maximal spectral bandwidth of the pulse parametrically amplified under the multi-beam pumping we have optimised the angles of pumping relative to the crystal axis and amplified radiation. The pump beams were considered pairwise because in the case of type-I phase matching one can choose two equal noncollinearity angles in the noncritical plane. Data on the angles are given in Table 2, where phase matching angles imply the angle between the pump beam and the crystal axes and the noncollinearity angle refers to the angle between the amplified beam and pump beam (the amplified beam and pump beam are schematically shown in Fig. 9). The intensities for each pump beam on a crystal are calculated by using the above consideration concerning combining of the pump beams and are presented in Table 3. The lengths of crystals providing a maximal energy are given in Table 4.

Table 2. Angular characteristics of multi-beam pumping.

Number of pairs of pump beams	Wavelength/nm	Noncolinearity angle/deg	Matching angle/deg
1	532	1.237	13.438
2	532	1.342	13.834
3	532	1.447	14.283

Based on the developed model we have calculated the energy and peak power of amplified pulses versus the number (from one to six) of the pump beams with the energy of 10 J at the duration of 90 ps and wavelength of 532 nm (Fig. 10). In the analysis, as input radiation was taken the radiation amplified after the third stage with the energy of ~100 mJ and duration of 10 fs. For one and two pump beams, the optimal noncollinearity angles and phase matching were, respectively, 1.33° and 13.77°; the first and second beam pairs were taken as two pairs of pump beams (see Fig. 9).

Note that if the pump wavelength is reduced from 532 to 527.5 or 515 nm, the results of these calculations as well as the noncollinearity angles and phase matching do not substantially change due to a small difference in the wavelengths.

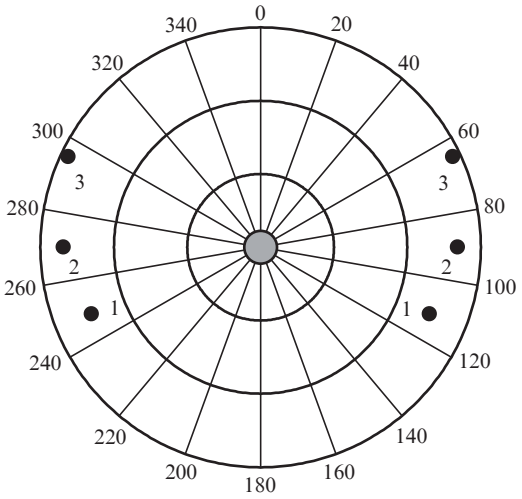

Figure 9. Schematic presentation of the amplified (central grey circle) and pump beams (black circles) in the far-field zone; digits are the numbers of pairs given in Table 2. The radial grid step is 0.5°, the projection of the plane XY of crystal is the vertical straight line.

Table 3. Intensities of radiation for coherent and incoherent pump beams in a LBO crystal.

Number of pump beams	Radiation intensity/ GW cm^{-2}	
	Coherent	Incoherent
1	8	8
2	2	4
4	0.5	2
6	0.22	1.33

Table 4. Lengths of LBO crystals for coherent and incoherent pump beams.

Number of pump beams	Crystal length/cm	
	Coherent	Incoherent
1	0.5	0.5
2	0.8	0.55
4	1.2	0.6
6	1.6	0.65

The spectra of amplified pulses for coherent and incoherent pump beams are presented in Fig. 11. The duration of amplified pulses calculated from the spectra of Fig. 11a (coherent pumping) weakly depend on the number of pump beams varying from 8.9 fs for one-beam pumping to 9.8 fs for four-beam pumping (the increase is explained by lower intensity and worse spectrum overlapping), and to 10.5 fs for six pump beams (the increase in comparison with four pump beams is due to the worse overlapping of spectra with the latter pair). In the case of incoherent pumping (Fig. 11) the range of pulse durations is 8.9–9.6 fs.

Similar calculations performed for DKDP crystal show the possibility of obtaining substantially lower energies and longer durations of amplified pulses, which is explained by the lower second-order nonlinearity and hence reduced amplification efficiency. Note that one possible problem in realising the multi-beam pumping in high-power amplification stages is the problem of introducing many pump beams into a nonlinear crystal. At small noncollinearity angles, the collimation of beams in the nonlinear crystal requires long

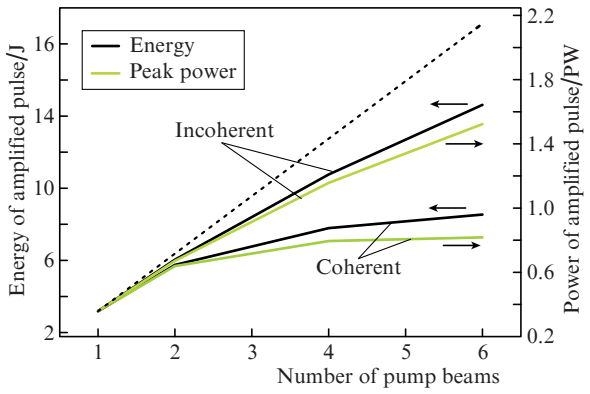

Figure 10. Energy and peak power of amplified pulses vs. the number of pump beams (parameters are given in the text); dotted line is the 'ideal' scaling (the energy and power of amplified beam are multiplied to the number of beams).

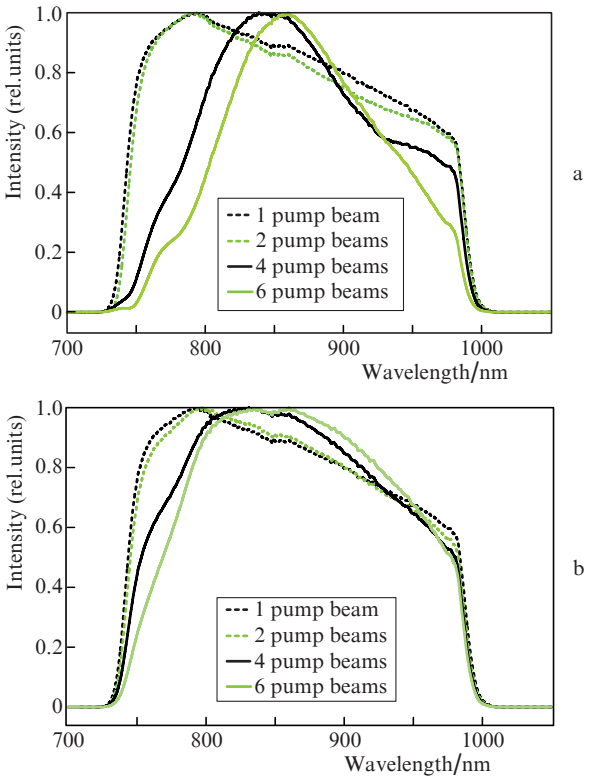

Figure 11. Gain profiles for (a) coherent and (b) incoherent pump beams.

distances and would worsen the angular stability of amplified radiation which is critical for systems with coherent combining [4].

Thus, the employment of six pump beams with the energy 10 J each provides possible amplification in an LBO crystal of up to 8 J (coherent beams) or 14 J (incoherent beams), which finally yields the amplification efficiency of 13% and 23%, respectively with its maximal possible value of 31%. The difference in the energies and especially in the peak power of amplified pulses between four and six coherent pump beams is minimal, that is, employment of more than four coherent pump beams in this configuration is not reasonable.

6. Conclusions

We have developed and fabricated a two-channel laser system which comprises three stages of wide-band parametric amplification based on BBO and LBO crystals in each channel and the system for stabilising the relative jitter of amplified pulses to 110 as. For the first time the coherent combining of two series of parametrically amplified femtosecond pulses with the energy of ~150 mJ and pulse repetition rate of 10 Hz has been experimentally realised. The efficiency of coherent combining was above 90%.

For the first time the modulation of the spectrum in amplifying wide-band femtosecond radiation in crystals placed in series has been experimentally observed which arises due to the phase sensitivity of parametric amplification and to noncollinearity of the waves participating in the process. The model has been developed for calculating the dependences of the period and modulation depth of the spectrum on the distance between crystals and on divergences of involved radiations. Results of the numerical simulation of parametric amplification in the frameworks of the model developed well agree with the data obtained experimentally.

The model of parametric luminescence evolution has been developed with diffraction, double refraction, dispersion of group velocities, and saturated amplification taken into account. The specific feature of the model is the possibility of calculating the whole range of the frequency-angular spectrum of amplified luminescence generated in the OPCPA. This feature makes it possible to estimate, in addition to contrast, the energy of superluminescence taking into account the whole range of angular and spectral components, which is important for optimising the amplification efficiency.

A series of experiments has been performed on measuring the contrast in the laser system with parametric amplification. It was established that results of calculating the contrast of amplified pulses by the model developed by us sufficiently well correspond to experimental data, which makes it possible to employ it for calculating and optimising the contrast of systems based on parametric amplification cascades. Based on the model developed, recommendations on improving the contrast of amplified pulses in the multi-terawatt laser system based on cascades of parametric amplification are presented.

Possible schemes have been analysed for employing the multi-beam pumping of output stages for obtaining the petawatt peak power of amplified pulses. It is shown that the petawatt level can be reached in the output stage of a parametric amplifier based on LBO crystal with employment of six incoherent pump beams with the energy of 10 J each.

Acknowledgements. The work was partially supported by the Programme of the Presidium of Russian Academy of Sciences 'Extreme Light Fields and Their Applications' and by the RF President's Grant for the State Support to the Leading Scientific Schools (Grant No. HSh-4096.2014). The authors acknowledge the Centre for Collective Use of 'Laser Femtosecond Complex' (Institute of Laser Physics, Siberian Branch of the Russian Academy of Sciences) for the hardware support.

References

1. Mourou G.A., Tajima T., Bulanov S.V. *Rev. Mod. Phys*., **78**, 309 (2006).
2. Lozhkarev V.V., Freidman G.I., et al. *Laser Phys. Lett*., **4**, 421 (2007).
3. Lu Xu, Lianghong Yu, et al. *Opt. Lett*., **38**, 4837 (2013).
4. Bagayev S.N., Trunov V.I., Pestryakov E.V., Frolov S.A., Leshchenko V.E., Kokh A.E., Vasiliev V.A. *Laser Phys*. (2014) (in press).
5. Leshchenko E.V., Trunov V.I., Pestryakov E.V., Frolov S.A. *Opt. Atmos. Okean*., **27**, 332 (2014).
6. Umstadter D. *Phys. Plasmas*, **8**, 1774 (2001).
7. Herrmann D., Veisz L., Tautz R., Tavella F., Schmid K., Pervak V., Krausz F. *Opt. Lett*., **34**, 2459 (2009).
8. Tavella F., Marcinkevčius A., Krausz F. *New J. Phys*., **8**, 219 (2006).
9. Mikhailova J.M., Buck A., Borot A., Schmid K., Sears C., Tsakiris G.D., Krausz F., Veisz L. *Opt. Lett*., **36**, 3145 (2011).
10. Pestryakov E.V., Petrov V.V., Trunov V.I., Frolov S.A., et al. *Proc. SPIE Int. Soc. Opt. Eng*., **7994**, 799425 (2011).
11. Bagayev S.N., Trunov V.I., Pestryakov E.V., Leshchenko V.E., et al. *Opt. Spektrosk*., **115**, 356 (2013).
12. Volosov V.D., Kalintsev A.G. *Pis'ma Zh. Tekhn. Fiz*., **2**, 373 (1976).
13. Smith A.V., Armstrong D.J., Alford W.J. *J. Opt. Soc. Am. B*, **15**, 122 (1998).
14. Dmitriev V.G., Tarasov L.V. *Prikladnaya nelineinaya optika* (Applied Nonlinear Optics) (Moscow: Fizmatlit, 2004) p. 290.
15. Frolov S.A., Trunov V.I., Pestryakov E.V., Leshchenko V.E. *Kvantovaya Elektron*., **43**, 481 (2013) [*Quantum Electron*., **43**, 481 (2013)].
16. Chwedenczuk J., Wasilewski W. *Phys. Rev*., **78**, 063823 (2009).
17. Manzoni C., Moses J., et al. *Opt. Express*, **19**, 8357 (2011).
18. Chwedenczuk J., Wasilewski W. *Phys. Rev. A*, **78**, 063823 (2008).
19. Klyshko D.N. *Fotony i nelineinaya optika* (Photons and Nonlinear Optics) (Moscow: Nauka, 1980) p.20.
20. Hong K.-H., Hou B., Nees J.A., et al. *Appl. Phys. B*, **81**, 447 (2005).
21. Tavella F., Schmid K., Ishii N., et al. *Appl. Phys. B*, **81**, 753 (2005).
22. Dorrer C., Begishev I.A., et al. *Opt. Lett*., **32**, 2143 (2007).
23. Antonetti A., Blasco F., et al. *Appl. Phys. B*, **65**, 197 (1997).
24. Mennerat G., Trophème B., Boulanger B., in *Nonlinear Optics*. B. Boulanger, S. Cundiff, M. Kauranen, W. Knox (Eds) *OSA Techn. Dig.* (online) (New York: OSA, 2013) p. NTu1B.1.
25. Ališauskas S., Butkus R., Pyragaitė V., Smilgevičius V., Stabinis A., Piskarskas A. *Opt. Commun*., **283**, 469 (2010).
26. Herrmann D., Tautz R., et al. *Opt. Express*, **18**, 4170 (2010).
27. Tamošauskas G., Dubietis A., et al. *Appl. Phys. B*, **91**, 305 (2008).
28. Marcinkevčius A., Piskarskas A., Smilgevičius V., Stabinis A. *Opt. Commun*., **158**, 101 (1998).